



Synthesis, crystal structures and biological evaluation of water-soluble zinc complexes of zwitterionic carboxylates

Jin-Xiang Chen^a, Wei-Er Lin^a, Chun-Qiong Zhou^a, Lee Fong Yau^c, Jing-Rong Wang^c, Bo Wang^b, Wen-Hua Chen^{a,*}, Zhi-Hong Jiang^{a,c,*}

^aSchool of Pharmaceutical Sciences, Southern Medical University, Guangzhou 510515, PR China

^bSchool of Chemistry and Chemical Engineering, Sun Yat-Sen University, Guangzhou 510275, PR China

^cSchool of Chinese Medicine, Hong Kong Baptist University, Kowloon Tong, Hong Kong

ARTICLE INFO

Article history:

Received 12 March 2011

Received in revised form 14 June 2011

Accepted 30 June 2011

Available online 18 July 2011

Keywords:

Zwitterionic carboxylates

Zinc(II) complexes

Crystal structures

DNA cleavage

Biological evaluation

ABSTRACT

Three water-soluble zinc complexes, $[\text{Zn}(\text{Cbp})_2\text{Br}_2]$ (**1**) (Cbp = *N*-(4-carboxybenzyl)pyridinium), $\{[\text{Zn}(\text{BCbpy})_2(\text{H}_2\text{O})_4]_3\text{Br}_6 \cdot 2(\text{BCbpy}) \cdot 2(4,4'\text{-bipy})\}$ (**2**) (BCbpy = 1-(4-carboxybenzyl)-4,4'-bipyridinium) and $\{[\text{Zn}_4(\text{Bpybc})_6(\text{H}_2\text{O})_{12}](\text{OH})_8 \cdot 9\text{H}_2\text{O}\}_{2n}$ (**3**) (Bpybc = 1,1'-bis(4-carboxybenzyl)-4,4'-bipyridinium), were synthesized and characterized by IR, elemental analysis and single-crystal X-ray crystallography. In complex **1**, the central Zn atom adopts a distorted tetrahedral coordination geometry that is formed from two unidentate Cbp ligands and two Br atoms. For complex **2**, the Zn atom in $[\text{Zn}(\text{BCbpy})_2(\text{H}_2\text{O})_4]^{2+}$ is strongly coordinated by four water molecules and two N atoms from two BCbpy ligands, hence forming an octahedral geometry. In complex **3**, each Bpybc ligand bridges two $[\text{Zn}(\text{H}_2\text{O})_3]^{2+}$ units through two terminal carboxylate groups in a monodentate coordination mode, thus forming a flowerlike two-dimensional network. Agarose gel electrophoresis (GE) and ethidium bromide (EB) displacement experiments indicated that complex **3** was capable of converting pBR322 DNA into open circular (OC) and linear forms, and exhibited high binding affinity toward calf-thymus DNA. MTT assay showed that complex **3** displayed inhibitory activities toward the proliferation of lung adenocarcinoma A549 and mouse sarcoma S-180 cells, with the IC_{50} values being 27.3 and 48.8 μM , respectively.

© 2011 Elsevier B.V. All rights reserved.

1. Introduction

It is well known that many metalloenzymes contain one or more zinc(II) ions in the active sites [1–3]. These Zn(II) ions generally show high affinity toward the oxygen atom(s) of carboxyl groups from carboxypeptidase [4]. Such zinc-containing active sites play a crucial role in the catalytic processes and have been characterized for their multiple activities [5,6]. Therefore, the chemistry of zinc complexes of carboxylates has been receiving an increasing attention. To date, a wide variety of model compounds has been prepared with the aim to mimic the structures and functions of the active sites of zinc metalloenzymes [7]. Remarkable among them are the biologically active compounds that are synthesized from Zn^{2+} and amino acid derivatives, for example, as anticonvulsant and antitumor agents and as synthetic nucleases [8,9].

Because zinc complexes having good water-solubility can find wide potential applications [10], considerable efforts have been spurred to develop their synthetic approaches [11–13]. One viable approach to improve the water-solubility of the resulting zinc complexes, is to incorporate carboxylate ligands with highly hydrophilic groups [13,14]. Herein, we report the synthesis, crystal structures and biological evaluation of water-soluble zinc complexes **1–3** of three zwitterionic carboxylates having quaternary ammonium groups, including *N*-(4-carboxybenzyl)pyridinium bromide (HCbpBr), 1-(4-carboxybenzyl)-4,4'-bipyridinium bromide (HBCbpyBr) and 1,1'-bis(4-carboxybenzyl)-4,4'-bipyridinium bromide ($\text{H}_2\text{BpybcBr}_2$) (Chart 1). Among them, it is reported that HCbpBr and HBCbpyBr have diverse coordination modes (Chart 2) [15–21].

2. Experimental

2.1. General

IR spectra were recorded on a Nicolet MagNa-IR 550. Elemental analyses for C, H, and N were performed on an EA1110 CHNS elemental analyzer. Electrospray ionization mass (ESI-MS) spectra

* Corresponding authors at: School of Pharmaceutical Sciences, Southern Medical University, Guangzhou 510515, PR China. Fax: +86 20 61648533 (W.-H. Chen), +852 34112461 (Z.-H. Jiang).

E-mail addresses: whchen@smu.edu.cn (W.-H. Chen), zhjiang@hkbu.edu.hk (Z.-H. Jiang).

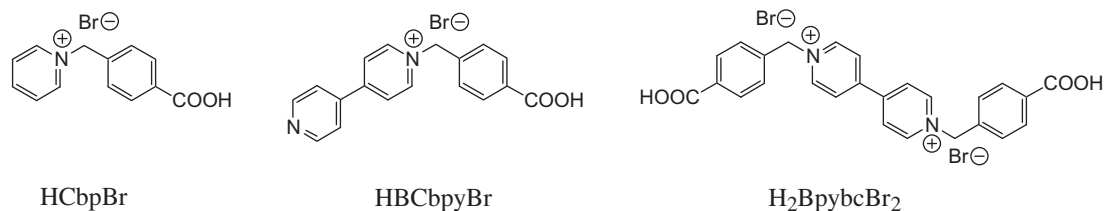


Chart 1. Chemical structures of HCbpBr, HBCbpyBr and H₂BpybcBr₂.

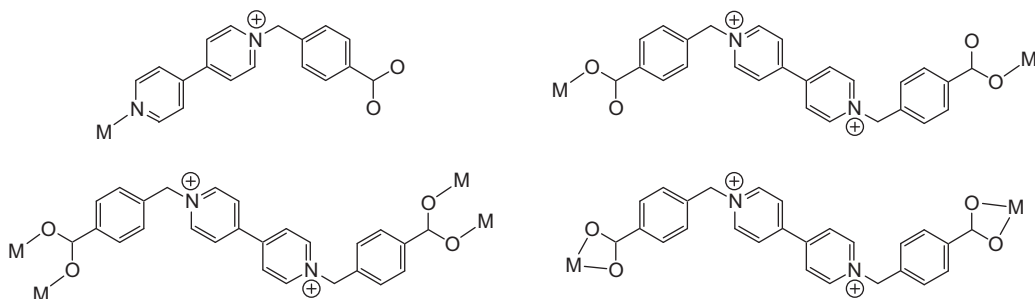


Chart 2. Reported coordination modes of HBCbpyBr and H₂BpybcBr₂.

were measured on an Applied Biosystems Sciex API 4000 Qtrap mass spectrometer. Agarose gel electrophoresis (GE) was conducted on DYY-8C electrophoresis apparatus and DYCP-31DN electrophoresis chamber, and detected on Alpha Hp 3400 fluorescence and visible light digital image analyzer. Fluorescence spectra were measured on a HITACHI F-2500 spectrofluorimeter.

Calf-thymus (CT) DNA and plasmid pBR322 DNA were obtained from Sigma–Aldrich and Takara Chemical Co., respectively. Their solutions were prepared in 5 mM Tris–HCl buffer (5 mM NaCl, pH 7.63). The concentration of CT DNA was determined spectrophotometrically using the molar extinction coefficient of $13\,200\text{ M}^{-1}\text{ cm}^{-1}$ per base pair (bp) at 260 nm [22]. HCbpBr, HBCbpyBr and H₂BpybcBr₂ were prepared according to the reported protocols [16,23,24]. All the other chemicals and reagents were obtained from commercial sources and used without further purification. Buffer solutions were prepared in triply distilled deionized water.

2.2. Synthesis of complexes 1–3

2.2.1. [Zn(Cbp)₂Br₂] (1)

HCbpBr (118 mg, 0.4 mmol) was dissolved in H₂O (5 mL), and the pH was adjusted to 7 with 0.1 M NaOH solution. Then, a solution of Zn(NO₃)₂·6H₂O (59 mg, 0.2 mmol) in H₂O (5 mL) was added. The resulting mixture was stirred for 30 min to give a clear solution, and then allowed to stand for 1 month to produce colorless blocks. Subsequent washing with Et₂O and drying under vacuum yielded **1** (63 mg, 48% based on HCbpBr). Elemental Anal. Calc. for C₂₆H₂₂Br₂ZnN₂O₄: C, 47.92; H, 3.40; N, 4.30. Found: C, 47.45; H, 3.37; N, 4.45%. IR (KBr disc, cm⁻¹) ν 1632 (w), 1594 (m), 1548 (w), 1507 (w), 1488 (w), 1416 (w), 1390 (w), 1374 (m), 1178 (w), 770 (m).

2.2.2. {[Zn(BCbpy)₂(H₂O)₄]₃Br₆·2(BCbpy)·2(4,4'-bipy)} (2)

To a solution of HBCbpyBr (149 mg, 0.4 mmol) in H₂O (5 mL) were added dropwise 0.1 M NaOH solution to adjust the pH 7, and then a solution of Zn(NO₃)₂·6H₂O (59 mg, 0.2 mmol) in H₂O (5 mL). The resulting mixture was stirred at room temperature for 1 h to give a clear solution, and then allowed to stand for 45 days to produce colorless blocks. Subsequent washing with Et₂O and drying under vacuum yielded **2** (133 mg, 76% based on HBCbpyBr).

Elemental Anal. Calc. for C₁₆₄H₁₅₂Br₆N₂₀O₂₈Zn₃·26.7H₂O: C, 49.15; H, 5.16; N, 6.99. Found: C, 49.78; H, 4.74; N, 6.82%. IR (KBr disc, cm⁻¹) ν 3446 (s), 3049 (w), 1614 (s), 1558 (w), 1456 (w), 1380 (s), 1158 (w), 811 (w), 744 (w).

2.2.3. {[Zn₄(Bpybc)₆(H₂O)₁₂](OH)₈·9H₂O}_{2n} (3)

Similar procedures for the synthesis of **2** were employed, except that H₂BpybcBr₂ (120 mg, 0.2 mmol) and Zn(NO₃)₂·6H₂O (59 mg, 0.2 mmol) in H₂O (5 mL) were used. Yield: 93 mg (82% based on H₂BpybcBr₂). Elemental Anal. Calc. for C₃₁₂H₃₄₀N₂₄O₁₀₆Zn₈: C, 56.39; H, 5.15; N, 5.06. Found: C, 55.91; H, 4.87; N, 4.92%. IR (KBr disc, cm⁻¹) ν 3400 (s), 3047 (s), 1616 (s), 1597 (s), 1556 (s), 1395 (s), 1374 (s), 1164 (m), 1019 (w), 1808 (m), 770 (w), 512 (w).

2.3. X-ray structures of complexes 1–3

All the measurements were made on a Rigaku Mercury CCD X-ray diffractometer by using graphite monochromated Mo K α ($\lambda = 0.71070\text{ \AA}$). Crystals of **1–3** were mounted with grease at the top of a glass fiber, and cooled at 193 K in a liquid nitrogen stream. Cell parameters were refined by using the program CrystalClear (Rigaku and MSC, Ver. 1.3, 2001). The collected data were reduced by using the program CrystalStructure (Rigaku and MSC, Ver. 3.60, 2004) while an absorption correction (multiscan) was applied.

The crystal structures of **1–3** were solved by direct methods and refined on F^2 by full-matrix least square methods with SHELXTL-97 program [25]. All non-hydrogen atoms were refined anisotropically, and all the hydrogen atoms were placed in geometrically idealized positions. For **2**, free 4,4'-bipy was found to disorder over two sites with an occupancy factor of 0.5/0.5 for N9/N9A, N10/N10A, C73/C73A, C74/C74A, C75/C75A, C76/C76A, C77/C77A, C78/C78A, C79/C79A, C80/C80A, C81/C81A and C82/C82A. The solvent accessible void occupies a volume of 781.0 \AA^3 (8.3% of the total cell volume) and is filled with highly disordered H₂O based on the FT-IR spectra. Because the disorder models did not give satisfactory results, the solvent contribution to the scattering factors was taken into account with PLATON/SQUEEZE [26]. As a result, a total of 267 electrons were found in each unit cell, corresponding to 26.7H₂O molecules per cell. Where relevant, the crystal data reported in this paper contained no contribution from the disordered

solvent molecules. Furthermore, the hydrogen atoms for the four disordered coordinated waters (O1W, O2W, O3W, and O4W) were not located. For **3**, the solvent accessible void occupies a volume of 352.0 Å³ (1.2% of the total cell volume) and may be due to the disorder of the solvent, because the largest electron-density peak is 1.793 e/Å³ and there are only eight electron-density peaks beyond 1. A summary of the key crystallographic information for **1–3** was tabulated in Table 1.

2.4. DNA cleavage experiments

The cleavage of supercoiled pBR322 DNA by complexes **1–3** was studied by agarose GE. The reaction was carried out by mixing DNA (0.35 g/L, 0.7 μL), the complex (4 mM, 9.8 μL) and 5 mM Tris–HCl buffer (5 mM NaCl, pH 7.63, 5.5 μL). The reaction mixture was incubated at 50 °C for 5 h, followed by the addition of loading buffer (4 μL) containing 0.035% bromophenol blue, 36% glycerol, 30 mM EDTA and 0.05% xylene cyanol FF to quench the reaction. The solution was then loaded on 1% agarose gel containing ethidium bromide (EB) (1.0 mg/L), and analyzed with electrophoresis in Tris–acetate–EDTA (TAE) buffer (pH 7.37). Bands were visualized by UV light and photographed. The probable cleavage mechanism was studied in a similar way, except in the presence of several scavengers, including H₂O₂ (1.0 mM), DMSO (0.4 M), glycerol (0.4 M) and MeOH (2.5 M).

2.5. DNA binding experiments

2.5.1. EB displacement experiments

EB displacement experiments of complexes **1–3** were performed at room temperature. As a typical example, to a solution of CT DNA (1.5 μM) and EB (3.8 μM) in 5 mM Tris–HCl (5 mM NaCl, pH 7.63) were added aliquots of complex **3** solution (0.2 M) in the same buffer containing CT DNA (1.5 μM) and EB (3.8 μM). The corresponding fluorescence spectra were measured ($\lambda_{\text{ex}} = 490 \text{ nm}$) until saturation was observed. The binding constants (K_{a} 's) were obtained by analyzing the relative fluorescence intensity (I/I_0) as a function of the concentrations of the added complexes **1–3** [27].

2.6. MTT assay

The cytotoxicities of complexes **1–3** were evaluated against human lung cancer cell line A549 and mouse sarcoma cancer cell line S180, by using MTT assay. The cells were cultured in DMEM (for A549) or RPMI (for S180) medium with 10% FBS. Exponentially growing cells were seeded into a 96-well plate at a density of 1.5×10^4 cells/well and allowed to adhere for 16 h before treatment (for A549 cells). Complexes **1–3** of varying concentrations were added to each vial and incubated for another 48 h. Then, MTT solution (5 mg/mL, 10 μL) was added to each well and incubated for 4 h at 37 °C. Then, lysing sodium dodecyl sulfate (SDS, 100 μL) was added and the resulting solution was kept overnight at room temperature. The optical densities were determined at 570 nm using a microplate reader. Dose–response curves were obtained and the results were expressed as IC₅₀ values in μM. Each experiment was carried out for three times, and the mean values were adopted.

3. Results and discussion

3.1. Crystal structures of complexes **1–3**

3.1.1. Complex **1**

It crystallizes in the tetragonal space group *I41cd* and the asymmetric unit consists of half of the [Zn(Cbp)₂Br₂] molecules. The

Table 1
Crystallographic data for **1–3**.

Complex	1	2	3
Molecular formula	C ₂₆ H ₂₂ Br ₂ N ₂ O ₄ Zn	C ₁₆₄ H ₁₂₈ Br ₆ N ₂₀ O ₂₈ Zn ₃	C ₃₁₂ H ₃₄₀ N ₂₄ O ₁₀₆ Zn ₈
Formula weight	651.65	3502.43	6645.04
Crystal system	tetragonal	monoclinic	hexagonal
Space group	<i>I41cd</i>	<i>P21/c</i>	<i>R3</i>
<i>a</i> (Å)	14.292(2)	21.989(3)	34.965(4)
<i>b</i> (Å)	14.292(2)	20.632(2)	34.965(4)
<i>c</i> (Å)	24.233(5)	20.891(2)	27.408(5)
β (°)		97.761(2)	
γ (°)			120.00
<i>V</i> (Å ³)	4949.9(14)	9390.9(18)	29018.0(7)
<i>Z</i>	8	2	3
<i>T</i> (K)	293(2)	110(2)	291(2)
<i>D</i> _{calc} (g cm ⁻³)	1.749	1.239	1.141
λ (Mo K α) (Å)	0.71073	0.71073	0.71073
μ (cm ⁻¹)	4.257	1.722	0.564
Total reflections	24 136	51 037	41 611
Unique reflections	2471	15 064	10 560
Number of observations	2870	20 371	31 210
Number of parameters	159	977	720
<i>R</i> ^a	0.0908	0.0805	0.0873
<i>wR</i> ^b	0.1604	0.1261	0.1584
Goodness-of-fit (GOF) on <i>F</i> ^{2c}	1.164	1.132	1.010
$\Delta\rho_{\text{max}}$ (e Å ⁻³)	1.579	2.766	1.793
$\Delta\rho_{\text{min}}$ (e Å ⁻³)	-1.454	-2.044	-1.702

^a $R = \sum ||F_o| - |F_c|| / \sum |F_o|$.

^b $wR = \{ \sum w(F_o^2 - F_c^2)^2 / \sum w(F_o^2)^2 \}^{1/2}$.

^c $GOF = \{ \sum w(F_o^2 - F_c^2)^2 / (n - p) \}^{1/2}$, where *n* = number of reflections and *p* = total numbers of parameters refined.

perspective view of **1** is shown in Fig. 1. It can be seen that there is a C₂ axis through the central Zn atom that is strongly coordinated by two unidentate Cbp ligands and two Br atoms, hence forming a distorted tetrahedral ZnO₂Br₂ coordination geometry in which two Cbp groups are oriented in the same directions. In addition, the Zn atom has weak interactions with two O atoms from the same two Cbp ligands. Such a structure closely resembles those of zinc complexes of carboxylate ligands, such as {ZnBr₂[HSC(CH₃)₂CH(NH₃)COO]₂} [28] and {ZnBr₂[NH₂COPY CH₂COO]₂} [29]. The coordinated Zn–O, Zn–Br and the pendant Zn···O bond lengths are 2.259(10), 2.634(2) and 2.620(8) Å, respectively. The bond angles around the zinc(II) atom lie in the range from 93.1(3)° to 148.5(6)°.

3.1.2. Complex **2**

It crystallizes in the monoclinic space group *P21/c* and the asymmetric unit consists of one and half discrete {[Zn(BCbpy)₂(-H₂O)₄] molecules, four Br⁻ anions (two of them having 0.5 occupancies), one discrete BCbpy molecule and one disordered 4,4'-bipy molecule. As depicted in Fig. 2, there are two almost identical but crystallographically independent molecules in complex **2**. In each molecular unit, the central Zn atom is strongly coordinated by four water molecules and two N atoms from two BCbpy ligands, thereby forming an octahedral geometry. Such a structure closely resembles that of the corresponding cobalt complex of BCbpy ligand [15]. The O atoms from carboxylate groups of the two coordinated BCbpy ligands have strong interaction with the O atoms from the coordinated water molecules in the adjacent complex units. Furthermore, the O atoms of the carboxylic groups from free BCbpy ligands have strong interaction with the O atoms of the coordinated water molecules from {[Zn(1)(BCbpy)₂(H₂O)₄] units, thus generating one-dimensional centipede-like structure as shown in

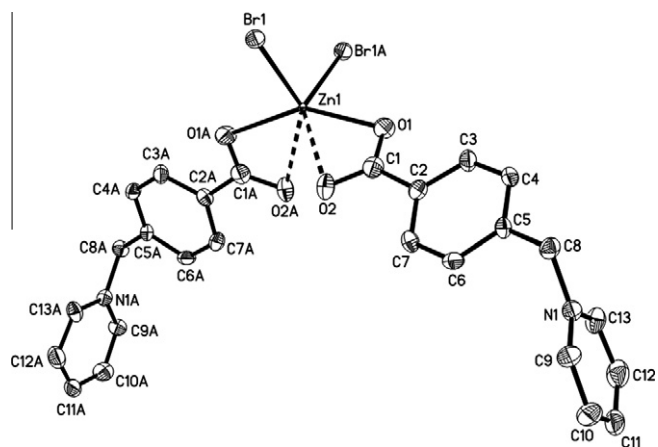


Fig. 1. Molecular structure of **1** with 50% thermal ellipsoids. All the hydrogen atoms are omitted for clarity. Symmetry transformations were used to generate equivalent atoms: A: $-x, -y + 2, z + 1$.

Fig. 3. Interestingly, its difference from the corresponding cobalt complex is that such chains are formed by alternating of every two $\{[\text{Zn}(1)(\text{BCbpy})_2(\text{H}_2\text{O})_4]\}$ units and one $\{[\text{Zn}(2)(\text{BCbpy})_2(-\text{H}_2\text{O})_4]\}$ unit. The contacts of $\text{Zn}(1) \cdots \text{Zn}(1\text{A})$ and $\text{Zn}(1) \cdots \text{Zn}(2\text{A})$ are 16.898 and 17.144 Å, respectively. The Zn–N and Zn–O distances are in the normal range of 2.135(6)–2.153(5) Å and 2.074(4)–2.115(4) Å, respectively.

3.1.3. Complex 3

It crystallizes in the hexagonal space group $R\bar{3}$ and the asymmetric unit consists of one third of the discrete $[\text{Zn}_4(\text{Bpybc})_6(\text{H}_2\text{O})_{12}]$ molecules, four OH^- (one of them having one third occupancies and two of them having two third occupancies) and seven solvated H_2O molecules (two of them having 0.5 occupancies and four of them having 0.25 occupancies). As shown in Fig. 4, there is a 3-fold axis located on the central Zn atom that is coordinated by three water molecules, thereby forming a $[\text{Zn}(\text{H}_2\text{O})_3]$ unit. Each Bpybc ligand bridges two $[\text{Zn}(\text{H}_2\text{O})_3]$ units through two terminal carboxylic groups in a monodentate coordination mode, thereby forming a flowerlike two-dimensional network as shown in Fig. 5. The Zn atoms adopt an octahedral coordination geometry. Because the methylene groups are used as knots to link the pyridyl and phenyl rings, the whole Bpybc ligand is not linear but exhibits a zigzag conformation. The two pyridyl rings of the 4,4'-bipyridyl group of Bpybc ligand are almost coplanar, whereas the phenyl rings are twisted significantly from the adjacent pyridyl ring, with a dihedral angle of $75.1(1)^\circ$. The linear distance between the two

terminal carboxylic groups is ca. 18.82 Å [16]. The Zn–O bond lengths are in the normal range.

3.1.4. Characterization of 1–3

Complexes **1–3** were further characterized by elemental analysis and IR. Firstly, complexes **1** and **3** gave elemental compositions that were consistent with their chemical formula. However, complex **2** afforded a slightly high error in carbon elemental analysis, possibly due to the loss of two solvated H_2O molecules during the course of sample preparation. In the IR spectra of **1–3**, the absence of any strong bands around 1700 cm^{-1} indicated that the carboxylic acid groups of three ligands were deprotonated. In addition, the asymmetric and symmetric stretching vibrations of the COO groups were observed at $1594/1390 \text{ cm}^{-1}$ for **1** and $1597/1395 \text{ cm}^{-1}$ for **3**, respectively. The difference in $\nu_{\text{as}}(\text{COO})$ and $\nu_{\text{s}}(\text{COO})$ ($\Delta = 204 \text{ cm}^{-1}$ for **1** and 202 cm^{-1} for **3**) suggests that the carboxylate groups coordinated to the metal ions only in a monodentate bridging mode. The stretching vibrations of the COO groups of **1** and **3** were shifted towards higher frequency compared with that (observed at $1558/1380 \text{ cm}^{-1}$) of the carboxylate group of **2**, suggesting that the carboxylate group of **2** was not coordinated to zinc ion [30].

3.2. Cleavage of pBR 322 DNA

It is well known that many metal complexes are capable of catalyzing the hydrolysis of DNA [7], therefore we investigated the cleaving activities of complexes **1–3** toward pBR322 DNA, by using agarose GE. Fig. 6 shows the GE patterns for the cleavage of pBR322 DNA by complexes **1–3** and their corresponding ligands at pH 7.63 and 50°C . It can be seen that complex **3** could relax the supercoiled form of DNA (CCC) to an open circular form (OC) (Lane 4), indicating that **3** was capable of cleaving pBR322 DNA. However, complexes **1** and **2** (Lanes 2 and 3), the three ligands (Lanes 5–7) and 4,4'-bipyridine (Lane 9) showed no cleaving activities. It should be noted that compared with pBR322 DNA itself (Lane 1), less Form II (OC) was observed in the presence of the three ligands and 4,4'-bipyridine. To gain insight into this phenomenon, we examined the morphological changes induced by heating pBR322 DNA from 37 to 50°C , as it is reported that thermal conversion of Form I (CCC) into Form II (OC) may occur [31]. As shown in Fig. S1, the amount of Form II (OC) increased with the increase in the temperatures (Lanes 1–3, Fig. S1), whereas slightly decreased with the increase in the concentrations of $\text{H}_2\text{BpybcBr}_2$ at 50°C (Lanes 4–6, Fig. S1). This result strongly suggested that the three ligands and 4,4'-bipyridine significantly retarded the thermal transition of pBR322 DNA from Form I (CCC) to Form II (OC) at 50°C , thus leading to the less presence of Form II.

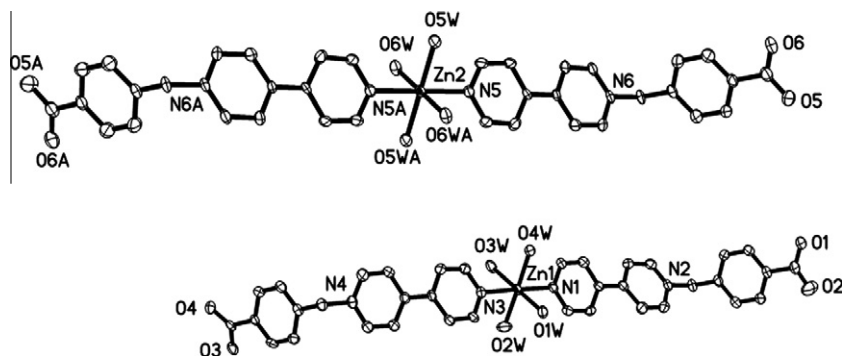


Fig. 2. Molecular structure of **2** showing two almost identical mononuclear building blocks. All the hydrogen atoms are omitted for clarity. Symmetry transformations were used to generate equivalent atoms: A: $-x + 1, -y + 2, z + 1$.

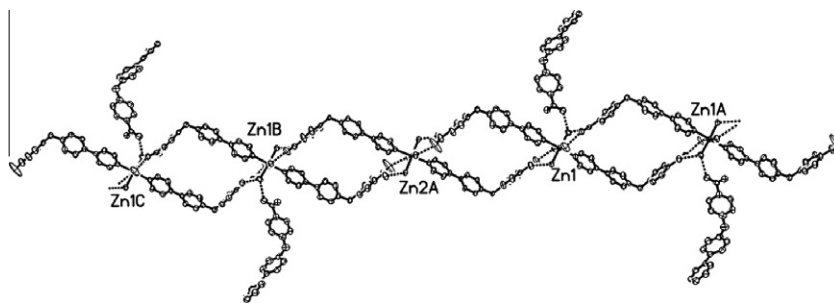


Fig. 3. One-dimensional double-stranded centipede-like structure formed by O...O contacts in **2**.

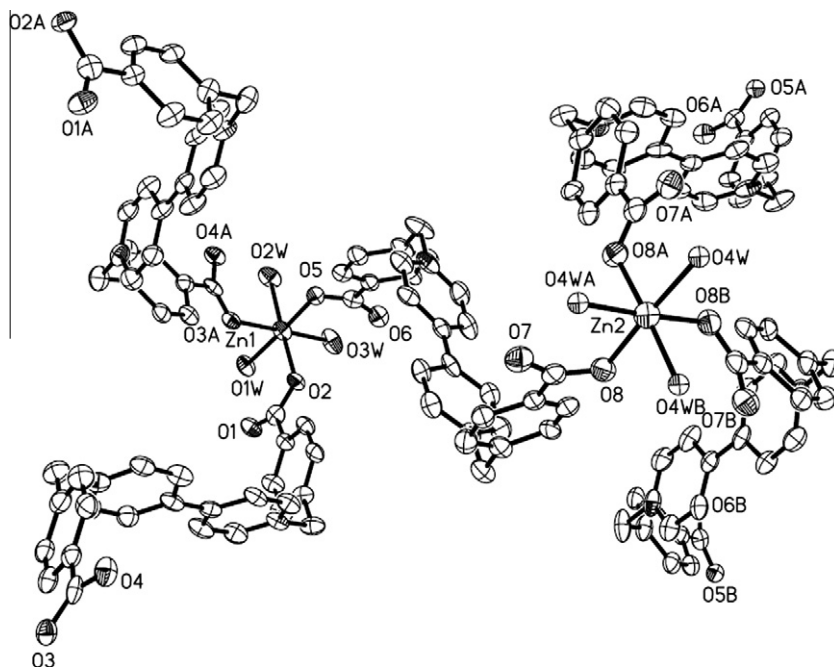


Fig. 4. Coordination environment of Zn(1) and Zn(2) in complex **3** with 50% thermal ellipsoids. All the hydrogen atoms are omitted for clarity. Symmetry transformations were used to generate equivalent atoms: A: $-x - y + 1, x + 1, -z$; B: $-x + y + 1, -x + 1, z$.

Then, we carried out the concentration-dependent DNA cleavage by **3** (Fig. 7). It is clear that the conversion of the supercoiled pBR322 DNA (Form I) to the nicked DNA (Form II) and linear DNA (Form III) was enhanced with the increase of the concentrations of complex **3** (Lanes 2–6), strongly suggesting that the cleavage was due to the presence of complex **3**.

It is known that nucleic acid can be cleaved through an oxidative or hydrolytic pathway. Therefore, to gain insight into the probable mechanism of action, we conducted the cleavage reactions in the presence of hydroxyl radical scavengers (DMSO, MeOH and glycerol) and an oxidant (H_2O_2) (Fig. S2) [32]. As a result, none of them had any influence on the DNA cleavage, strongly suggesting that hydroxyl radical was not involved in the DNA cleavage and that the cleavage might proceed via a hydrolytic rather than oxidative mechanism.

The aforementioned observation may be rationalized by taking into consideration the difference in the structures of complexes **1–3**. It is known that binding is a crucial step for DNA cleavage [13], and that polynuclear metal complexes generally have potent catalytic activity in DNA hydrolysis [7]. Complex **3** is composed of Bpybc ligands having two positive charges, and thus, should show higher DNA binding affinity than complexes **1** and **2**, because of its stronger electrostatic interaction with DNA. This and the polynuclear nature

may be the predominant factors for the higher DNA cleaving activity of complex **3**.

To verify these hypotheses, we firstly detected complex **3** in aqueous solution by means of ESI mass spectrometry. As shown in Fig. S3, one ion peak at m/z at 705.7 was observed, which was assignable to $[\text{Zn}_4(\text{Bpybc})_6(\text{H}_2\text{O})-4\text{H}]^{4+}$. For further characterization of the dissociation patterns of this abundant fragment ion, the multiple stage mass spectrometric measurements were carried out (Fig. S4). This ion was dissociated dominantly to the ion peaks at m/z 425.5 and 292.1, which were assignable to $([\text{HBpybc}]^+)$ and $([\text{HBCbpy}+\text{H}]^+)$, respectively. These results strongly suggested that the cluster **3**, or the core $[\text{Zn}_4(\text{Bpybc})_6]$ fragment remained in water solution.

To evaluate how strongly these complexes interact with DNA, we measured the binding affinities toward CT DNA of complexes **1–3** by means of EB displacement experiment. It is well known that EB can intercalate non-specifically into DNA. Competitive binding of other drugs to DNA leads to the displacement of bound EB and a decrease in the fluorescence intensity [33]. Addition of complex **1** led to slight quenching, suggesting that its interaction with CT DNA was very weak (Fig. 8). Both complexes **2** and **3** were capable of substituting EB bound to CT DNA, however, the latter was much more effective. Nonlinear fitting analyses of the relative fluorescence intensity

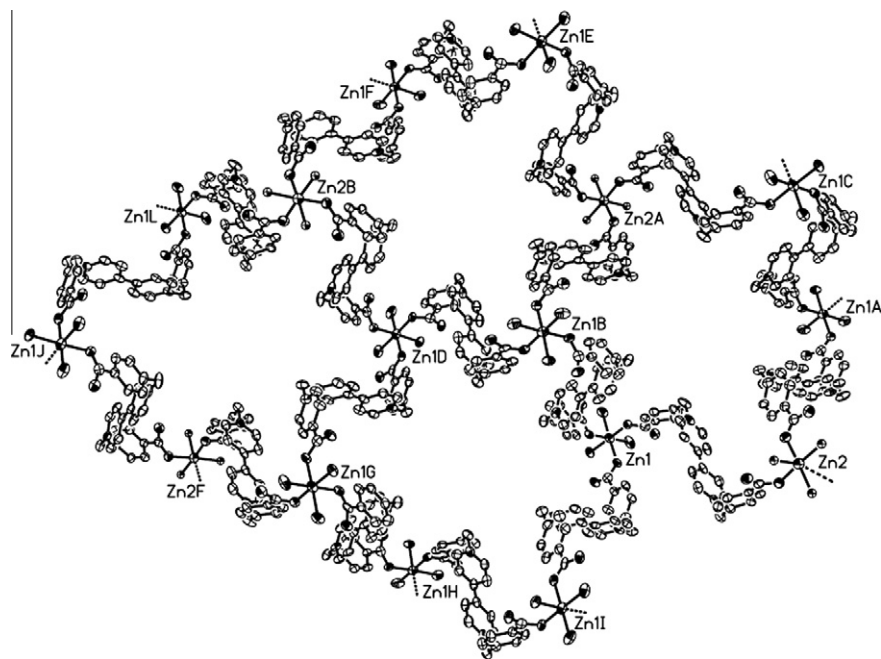


Fig. 5. Extended flowerlike two-dimensional network structure of **3**.

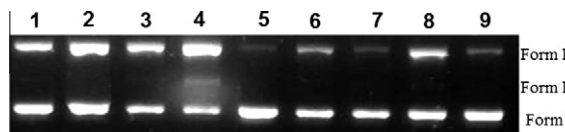


Fig. 6. Agarose GE patterns for the cleavage of pBR322 DNA by **1–3** and their corresponding ligands (3.85 mM) at pH 7.63 and 50 °C. Lane 1: DNA alone; Lanes 2–9: DNA with **1**, **2**, **3**, HCbpBr, H₂BpybcBr₂, HBCbpyBr, Zn²⁺, and 4,4'-bipy, respectively.

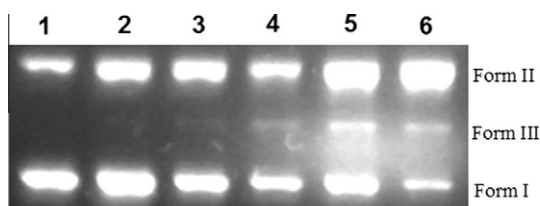


Fig. 7. Agarose GE patterns for the cleavage of pBR322 DNA by **3** of increasing concentrations at 50 °C and pH 7.63. Lane 1: DNA alone; Lanes 2–6: 0.3, 0.6, 1.2, 2.4 and 3.6 mM of **3**, respectively.

(I/I_0) as a function of the concentrations of added **2** and **3** afforded their binding constants being $(2.55 \pm 0.50) \times 10^4 \text{ M}^{-1}$ and $(4.28 \pm 2.79) \times 10^5 \text{ M}^{-1}$, respectively.

3.3. Biological activity

To exploit the potential application of complexes **1–3**, we evaluated their biological activities against human lung cancer A549 and mouse sarcoma cancer S180, by using MTT assay [34,35]. Table 2 lists the IC_{50} values of complexes **1–3** and their corresponding ligands. It can be seen that complexes **1** and **2** and all the ligands were inactive under our assay conditions, whereas complex **3** exhibited moderate inhibitory activity with the IC_{50} values being 27.3 μM toward lung adenocarcinoma A549 cells and 48.8 μM toward mouse sarcoma S-180 cells, respectively. This result was in agreement with their above-mentioned DNA cleavage activity.

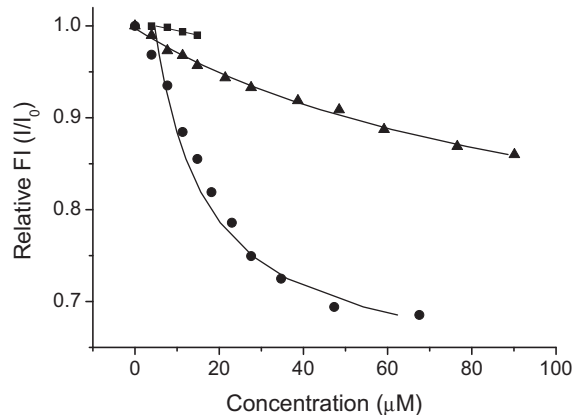


Fig. 8. Fluorescence decrease of EB (3.8 μM) induced by the competitive binding of **1** (■), **2** (▲) and **3** (●) to CT DNA (1.5 μM) in 5 mM Tris-HCl buffer (5 mM NaCl, pH 7.63) at room temperature ($\lambda_{\text{ex}} = 490 \text{ nm}$, $\lambda_{\text{em}} = 594 \text{ nm}$).

Table 2

Cytotoxicities (IC_{50} , μM) of complexes **1–3** and their corresponding ligands.

Complex	S180	A549	Complex	S180	A549
1	>100	>100	HCbpBr	>100	>100
2	>100	98.8	HBCbpyBr	>100	>100
3	27.3	48.8	H ₂ BpybcBr ₂	>100	>100

4. Conclusions

In summary, three water-soluble zinc complexes of zwitterionic carboxylates have been synthesized and characterized by IR, elemental analysis and single-crystal X-ray crystallography. EB displacement and GE experiments indicated that complex **3** displayed moderate ability to bind CT DNA and to cleave plasmid pBR322 DNA from supercoiled to nicked and linear forms. In addition, biological study indicated that complex **3** could inhibit the proliferation of lung adenocarcinoma A549 and mouse sarcoma

S-180 cells with the IC₅₀ values being 27.3 and 48.8 μM, respectively. These findings may provide some useful guidance for the future design and synthesis of water-soluble zinc complexes with potent biological activities, which is currently under active investigation in our laboratories.

Acknowledgments

This work was financially supported by the Medical Scientific Research Foundation (No. B107) and the Department of Education of Guangdong Province of China, the International Science and Technology Cooperation Base of Southern Medical University (2010JD035) and Southern Medical University.

Appendix A. Supplementary material

CCDC 804539, 804540, and 804541 contain the supplementary crystallographic data for **1**, **2**, and **3**. These data can be obtained free of charge from The Cambridge Crystallographic Data Centre via www.ccdc.cam.ac.uk/data_request/cif. Supplementary data associated with this article can be found, in the online version, at [doi:10.1016/j.ica.2011.06.054](https://doi.org/10.1016/j.ica.2011.06.054).

References

- [1] H.J. Smith, C. Simons (Eds.), *Enzymes and their Inhibition Drug Development*, CRC Press, Boca Raton, London, New York, 2005, p. p. 1.
- [2] A. Innocenti, A. Scozzafava, C.T. Supuran, *Bioorg. Med. Chem. Lett.* 16 (2006) 4316.
- [3] S. Aoki, E. Kimura, *Chem. Rev.* 104 (2004) 769.
- [4] C. Temperini, A. Innocenti, A. Guerri, A. Scozzafava, S. Rusconi, C.T. Supuran, *Bioorg. Med. Chem. Lett.* 17 (2007) 2210.
- [5] Y. Tanaka, I. Grapsas, S. Dakoji, Y.J. Cho, S. Mobashery, *J. Am. Chem. Soc.* 116 (1994) 7475.
- [6] D.G. Xu, H. Guo, *J. Am. Chem. Soc.* 131 (2009) 9780.
- [7] C.L. Liu, M. Wang, T.L. Zhang, H.Z. Sun, *Coord. Chem. Rev.* 248 (2004) 147.
- [8] A. Tarushi, C.P. Raptopoulou, V. Psycharis, A. Terzis, G. Psomas, D.P. Kessissoglou, *Bioorg. Med. Chem.* 18 (2010) 2678.
- [9] J. d'Angelo, G. Morgant, N.E. Ghermani, D. Desmaële, B. Fraisse, F. Bonhomme, E. Dichi, M. Sghaier, Y.L. Li, Y. Journaux, J.R.J. Sorenson, *Polyhedron* 27 (2008) 537.
- [10] M. Baldini, M. Belicchi-Ferrari, F. Bisceglie, S. Capacchi, G. Pelosi, P. Tarasconi, *J. Inorg. Biochem.* 99 (2005) 1504.
- [11] I. Mopelola, N. Tebello, *Polyhedron* 28 (2009) 416.
- [12] Z.Y. Guo, P. Orth, S.C. Wong, B.J. Lavey, N.Y. Shih, X.D. Niu, D.J. Lundell, V. Madison, J.A. Kozlowski, *Bioorg. Med. Chem. Lett.* 19 (2009) 54.
- [13] S.A. Galal, K.H. Hegab, A.M. Hashem, N.S. Youssef, *Eur. J. Med. Chem.* 45 (2010) 5685.
- [14] J. Qian, X.F. Ma, J.L. Tian, W. Gu, J. Shang, X. Liu, S.P. Yan, *J. Inorg. Biochem.* 104 (2010) 993.
- [15] Q.X. Yao, Z.F. Ju, W. Li, W. Wu, S.T. Zheng, J. Zhang, *CrystEngComm* 10 (2008) 1299.
- [16] Y.Q. Sun, J. Zhang, Z.F. Ju, G.Y. Yang, *Cryst. Growth Des.* 5 (2005) 1939.
- [17] Q.X. Yao, W.M. Xuan, H. Zhang, C.Y. Tua, J. Zhang, *Chem. Commun.* (2009) 59.
- [18] Q.X. Yao, X.H. Jin, Z.F. Ju, H.X. Zhang, J. Zhang, *Cryst. Eng. Commun.* 11 (2009) 1502.
- [19] H.X. Zhang, Q.X. Yao, X.H. Jin, Z.F. Ju, J. Zhang, *Cryst. Eng. Commun.* 11 (2009) 1807.
- [20] Q.X. Yao, L. Pan, X.H. Jin, J. Li, Z.F. Ju, J. Zhang, *Chem. Eur. J.* 15 (2009) 11890.
- [21] Q.X. Yao, Z.F. Ju, X.H. Jin, J. Zhang, *Inorg. Chem.* 48 (2009) 1266.
- [22] M.E. Reichmann, S.A. Rice, C.A. Thomas, P.J. Doty, *J. Am. Chem. Soc.* 76 (1954) 3047.
- [23] J. Pícha, R. Cibulka, F. Liška, P. Parík, O. Pytela, *Collect. Czech. Chem. Commun.* 69 (2004) 2239.
- [24] K. Uemura, K. Saito, S. Kitagawa, H. Kita, *J. Am. Chem. Soc.* 128 (2006) 16122.
- [25] G.M. Sheldrick, *SHELX-97 and SHELXL-97*, Program for Crystal Structure Refinement, University of Göttingen, Germany, 1997.
- [26] A.L. Spek, *J. Appl. Crystallogr.* 36 (2003) 7.
- [27] J.Y. Pang, Y. Qin, W.H. Chen, G.A. Luo, Z.H. Jiang, *Bioorg. Med. Chem.* 13 (2005) 5835.
- [28] P. Bell, W.S. Sheldrick, *Z. Naturforsch. Teil B* 39 (1984) 1732.
- [29] V. Zelenak, K. Gyoryova, I. Cisarova, *Main Group Met. Chem.* 18 (1995) 211.
- [30] K. Nakamoto, *Infrared and Raman Spectra of Inorganic and Coordination Compounds*, John Wiley and Sons, New York, 1986.
- [31] H. Uedaira, S. Kidokoro, S. Ohgiya, K. Ishizaki, N. Shinriki, *Thermochim. Acta* 232 (1994) 7.
- [32] O.I. Aruoma, B. Halliwell, M. Dizdaroglu, *J. Biol. Chem.* 264 (1989) 13024.
- [33] D.D. Qin, Z.Y. Yang, B.D. Wang, *Spectrochim. Acta, Part A* 68 (2007) 912.
- [34] B. Liu, H. Chen, Z.Y. Lei, P.F. Yu, B. Xiong, *J. Asian Nat. Prod. Res.* 8 (2006) 241.
- [35] W. Wang, Q.L. Guo, Q.D. You, K. Zhang, Y. Yang, J. Yu, W. Liu, L. Zhao, H.Y. Gu, Y. Hu, Z. Tan, X.T. Wang, *Biol. Pharm. Bull.* 29 (2006) 1132.